Dynamical resonance tunnelling—a theory of giant emission from carbon field emitters

2005 J. Phys.: Condens. Matter 17 1505

(http://iopscience.iop.org/0953-8984/17/10/007)

INSTITUTE OF PHYSICS PUBLISHING JOURNAL OF PHYSICS: CONDENSED MATTER

J. Phys.: Condens. Matter **17** (2005) 1505–1528 doi:10.1088/0953-8984/17/10/007

Dynamical resonance tunnelling—a theory of giant emission from carbon field emitters

T C Choy, A M Stoneham and A H Harker

Department of Physics and Astronomy, University College London, Gower Street, London WC1E 6BT, UK

E-mail: a.harker@ucl.ac.uk

Received 24 December 2004, in final form 24 December 2004
Published 25 February 2005
Online at stacks.iop.org/JPhysCM/17/1505

Abstract

We describe in this paper the likely physical mechanisms that underlie the enormously enhanced electron emission observed from certain carbon field emitters. Our key ideas link the enhancement to dynamic resonant tunnelling and to the image interaction in a more general form than is usual. We have recently proposed a giant enhancement of the dynamic surface potential that could explain the anomalously large field emission currents observed in carbon-based emitters with predominantly non-Fowler–Nordheim I–V characteristics. Here we report further results on this effect which can best be described as an image-induced dynamical resonant tunnelling phenomenon, and in particular the applied field dependence of the inverse potential enhancement factor $\kappa(\omega)$, which seems to be a hallmark of such systems. The latter is studied by a consideration of the non-linear second-order susceptibility $\gamma(\omega)$ which couples the static applied field to the dynamic field. We derive the criterion for this mechanism to operate and demonstrate that it does indeed provide the linear field dependence of $\kappa(\omega)$ found in our earlier work. We further provide a link between $\gamma(\omega)$ and other microscopic parameters of the surface plasmon model, notably the anharmonicity coefficient, via a Duffing oscillator model. Through the use of a one-dimensional fluctuating barrier model with a self-consistent approach, we further assess the significance of other non-linear damping effects.

1. Introduction

We describe in this paper the likely physical mechanisms that underlie the enormously enhanced electron emission observed from certain carbon field emitters. Our key ideas link the enhancement to an image-induced dynamical resonant tunnelling phenomenon in a more general form than conventional theories. In a recent work [1] we have identified what appears to be a dynamical Schottky barrier lowering mechanism, operative in the case of carbon systems, that profoundly influences their efficiency for the field emission of electrons, most unlike

normal metal surfaces [2, 3]. This mechanism, while not fully understood at that time, has allowed us to model the field emission of certain carbon-based field emission systems such as graphitized carbon nano-tubes (CNTs) and PFE emitters, that lie outside the scope of traditional Fowler–Nordheim (FN) theory [1]. Its intriguingly excellent agreement with experimental data stimulated further thinking which this paper hopes to clarify. In our earlier work we have noted that the observed currents are too large for FN theory [1] and could not be fixed by minor adjustment of the local field enhancement factor β, such as the value of $\beta = 350$ as used in [1], or higher such as $\beta = 5 \times 10^3$ as used in [4–6]. The major problem with such a simplistic β factor theory is that of energy conservation. An electron emitted under such a local field (with $\beta = 350$ and $V = 20$ V μm^{-1} say) would gain a rather substantial energy of 0.7 eV (which must come from somewhere) by merely traversing a microscopic distance of 1 Å from the surface. With a $\beta = 5 \times 10^3$, this increases to a highly unreasonable energy of 10 eV, which makes a field enhancement factor theory somewhat dubious on its own.

In our earlier work [1] we gave a soluble model which allowed for a lowering of the barrier for emission for a subset of electrons near the Fermi level. The model was phenomenological rather than deduced systematically from any obvious physical assumptions. Its intriguingly good agreement with experimental data, and a closer examination of the proposed inverse potential enhancement factor κ, prompted us to suggest that the underlying mechanism is a dynamic one. There we also found evidence that the non-linear dynamic dielectric properties might be involved and we called for an urgent formulation of time-dependent quantum tunnelling theory of field emission. In fact our model was motivated by the fact that the substantial barrier reduction needed (from eVs to meVs) to obtain the order of magnitude tunnelling current found in carbon emitters can only make sense dynamically. Any static model with such huge barrier reductions would lead to a massive thermionic current at room temperatures ($J_T \sim AT^2 \mathrm{e}^{-\phi/k_\mathrm{B}T} \approx 10^7$ A cm^{-2}), which is clearly not observed. In this paper we shall report on our results, which show how an image-induced dynamical resonant tunnelling model can lead to the features found.

The conditions needed to give meaning to our model of enhanced tunnelling demand certain features of dynamical screening response to a tunnelling electron at the surface. Whilst we have to make several working approximations, these do not appear to be exotic in any way, although there are still important issues that will require further extensive studies which this work should motivate. More importantly, we have now been able to identify key parameters in the model that make carbon emitters different and do not behave in the FN-like metallic way. As a consequence we find that there may be opportunities for surface engineering to optimize field emission or indeed exploit the surface-plasmon features found for other device technologies such as THz generation. The reader should first bear in mind that, throughout this paper, the electric field F will often be compared with the characteristic *Schottky barrier field* $F_\mathrm{b} = 694\varphi^2$ V/μm (eV)$^{-2}$, where φ is the work function in eV.

Sections 2 and 3 derive expressions for the electron self-energy, the image interaction, and the tunnel current. The derivations, which are more general than usual, include working approximations that are discussed in detail. The generality is especially important when the Fermi energy is close to the surface plasmon resonance, the regime that makes possible the enhancement of the tunnel current. Non-linear terms are a further important factor, coupling the static applied field and the dynamic field due to the tunnelling electron (section 5). Experiment suggests that such non-linear terms are large for carbon systems; in principle, they can be measured by THz spectroscopy.

In three places we shall use simple models to get to grips with issues that can be both complex and subtle. Section 4 uses the classical Drude model to understand the dynamics of resonance and derive an effective Q-factor for the resonance. Section 6 exploits the

Duffing model, showing that the non-linear susceptibility is related to the anharmonicity of the surface plasmon. In section 7, we adopt a simple (fluctuating barrier) model to assess the self-consistency of the dielectric function, and find that enhancement through the non-linear coupling exceeds suppression from damping. The Drude model indicates that resonant tunnelling is unlikely in metals, for which collision times are too short. For the carbons, resonant tunnelling appears possible.

These ingredients are all brought together in section 8 to give an expression for the tunnel current (equation (88)) in terms of the non-linear coupling $\gamma(\omega_s)$, the work function φ, the electron affinity χ, the Schottky barrier field F_b (which itself is determined by φ) and the applied field F. This final equation is consistent with our earlier phenomenological model, and suggests that giant electron emission is likely to need low electron densities (if true!). The significant differences between the carbons showing enhanced emission and metals result from three factors: the closeness of Fermi energy and surface plasmon energy, the large non-linear coupling, and the relatively long collision times in the carbons.

2. Time-dependent theory of field emission

In this section we shall formulate precisely the time-dependent Schrödinger equation for the tunnelling electron interacting with its own image potentials. The exact one-particle non-retarded Hamiltonian $\hat{H}$ which provides the time-evolution of the electron's wavefunction during the tunnelling process can in principle be written down in the following way:

$$\mathrm{i}\hbar\frac{\partial\psi(\mathbf{r},t)}{\partial t} = \hat{H}\psi(\mathbf{r},t), \tag{1}$$

where the operator $\hat{H}$ is given by:

$$\hat{H}\psi(\mathbf{r},t) = -\frac{\hbar^2}{2m}\nabla^2\psi(\mathbf{r},t) + V_0(x)\psi(\mathbf{r},t) - \frac{e}{2}\Phi_1(\mathbf{r},F,t)\psi(\mathbf{r},t) - \frac{e}{2}\int_{-\infty}^{t}\mathrm{d}t'\Phi_2(\mathbf{r},F,t-t')\psi(\mathbf{r},t'). \tag{2}$$

Here we have as before:

$$V_0(x) = -\mu\Theta(-x) + (\varphi - eFx)\Theta(x), \tag{3}$$

in which the zero of energy is taken as the Fermi level (see also equation (1) of [1]), where F is the applied static external field, $\Theta(x)$ is the Heaviside step function, $\mu = (\chi - \varphi)$ where χ is the electron affinity and φ is the work function. In the above we have explicitly denoted the external applied field F dependence in the induced image potentials Φ_1 and Φ_2, which we shall suppress from now on for brevity, except when emphasis becomes necessary. Note that equation (3) can be modified to incorporate intermediate states quite easily, such as a shallow well with possible resonant levels. In this case the first term can be modified to incorporate this feature so that:

$$V_0(x) = -[\mu\Theta(-x-a_s) + \mu_s\Theta(x+a_s)]\Theta(-x) + (\varphi - eFx)\Theta(x), \tag{4}$$

where a_s is the width and $\mu_s < \mu$ is the depth of such a well. Such refinements do not alter the picture in a significant way, since its effect is to redefine the equilibrium chemical potential and so we will not look into this modification further. We must stress at the outset that in view of the time-dependent interactions the wavefunctions $\psi(\mathbf{r},t)$ are in general complex. Only stationary states can have real wavefunctions $\psi(\mathbf{r},t)$ (up to a trivial constant of unit modulus) [7].

2.1. Image potentials and self-energy

At this stage the induced image potentials Φ_1 and Φ_2 remain undefined[1]. To do so explicitly would require a full consideration of all the many-body interactions, such as electron–electron, electron–plasmon and electron–phonon, etc, to which the tunnelling electron can couple. Nevertheless, in the many-body language we can, following Jonson [8], formally write these potentials as:

$$\Phi_1(\mathbf{r}, t) = \int \mathrm{d}\mathbf{r}' \left[\frac{\Sigma_1(\mathbf{r}, \mathbf{r}', t)\psi(\mathbf{r}', t)}{\psi(\mathbf{r}, t)} \right], \tag{5}$$

where $\Sigma_1(\mathbf{r}, \mathbf{r}', t)$ is the instantaneous part of the non-local self-energy. In the same way:

$$\Phi_2(\mathbf{r}, t - t') = \int \mathrm{d}\mathbf{r}' \left[\frac{\Sigma_2(\mathbf{r}, \mathbf{r}', t - t')\psi(\mathbf{r}', t')}{\psi(\mathbf{r}, t')} \right], \tag{6}$$

in which $\Sigma_2(\mathbf{r}, \mathbf{r}', t - t')$ is the non-local and non-instantaneous part of the self-energy.

Without going into the many-body Hamiltonian, there are some general considerations that can be made, which motivate the form of equation (2) and define various symmetry relations. The operator $\hat{H}$ must be Hermitian in order that the time-evolution of the wavefunction is unitary. This implies first of all that the exact interaction potential $\Phi_1(\mathbf{r}, t)$, whose origin is electromagnetic, must be real:

$$\Phi_1(\mathbf{r}, t) = \Phi_1^*(\mathbf{r}, t), \tag{7}$$

or alternatively, the self-energy $\Sigma_1(\mathbf{r}, \mathbf{r}', t)$ satisfy the Hermitian property:

$$\Sigma_1^*(\mathbf{r}, \mathbf{r}', t) = \Sigma_1(\mathbf{r}', \mathbf{r}, t). \tag{8}$$

However, the non-instantaneous potential $\Sigma_2(\mathbf{r}, \mathbf{r}', t - t')$ cannot be real in general. Both it and the wavefunctions must satisfy the following convolution Hermitian property:

$$\int_0^\infty \mathrm{d}\tau\ \psi(\mathbf{r}, t)\Phi_2^*(\mathbf{r}, \tau)\psi^*(\mathbf{r}, t - \tau) = \int_0^\infty \mathrm{d}\tau\ \psi^*(\mathbf{r}, t)\Phi_2(\mathbf{r}, \tau)\psi(\mathbf{r}, t - \tau), \tag{9}$$

with a corresponding relation on the self-energy:

$$\int_0^\infty \mathrm{d}\tau\ \psi(\mathbf{r}, t)\Sigma_2^*(\mathbf{r}, \mathbf{r}', \tau)\psi^*(\mathbf{r}', t - \tau) = \int_0^\infty \mathrm{d}\tau\ \psi^*(\mathbf{r}', t)\Sigma_2(\mathbf{r}', \mathbf{r}, \tau)\psi(\mathbf{r}, t - \tau). \tag{10}$$

For this reason we have thus separated the instantaneous and the history-dependent terms, in anticipation that the theory may be cast in the form of spatial and frequency dispersive dielectric functions which must satisfy causality requirements. It must be noted that the above symmetry and causality requirements are not obtained for free. Any approximation scheme that does not satisfy one of these properties violates unitarity and will ultimately lead to errors in the calculation of the tunnelling current (see below). In a full many-body theory, a necessary (but not sufficient) condition is the requirement of so-called Ward–Takahashi identities [9]. For our purpose, the complex structure of $\Phi_2(\mathbf{r}, t)$ implies that its physical property is of quantum origin and therefore *cannot* in general be derived from classical electrodynamics alone, for which all electromagnetic potentials are real. This observation appears to agree with the sentiments of Mills in relation to inelastic energy losses [10]. Indeed equation (10) shows that the image potential equation (9) contains hidden quantum dynamical information that are imposed on it by unitarity.

[1] Note that we use the term potential in a general sense and not in the canonical sense of classical mechanics. This does pose deeper problems as to whether our theory can be derived through a Schrödinger canonical quantization procedure, which we shall ignore in our work.

Now we can utilize partial Fourier transforms so that all functions in space and time can be written as[2]:

$$\psi(x, \mathbf{R}, t) = \int \frac{\mathrm{d}\mathbf{K}}{(2\pi)^2} \int_{-\infty}^{\infty} \frac{\mathrm{d}E}{2\pi\hbar} \mathrm{e}^{-\mathrm{i}Et/\hbar} \mathrm{e}^{\mathrm{i}\mathbf{K}\cdot\mathbf{R}} \psi(x, \mathbf{K}, E), \tag{11}$$

where all bold vector quantities belong to the perpendicular y–z surface plane, and the usefulness of defining the zero of energy at the Fermi level as in equations (2) and (3) becomes apparent. Then the time-dependent Schrödinger equation becomes:

$$\begin{aligned} E\psi(x, \mathbf{K}, E) = {} & \left(-\frac{\hbar^2}{2m} \frac{\partial^2}{\partial x^2} + \frac{\hbar^2 K^2}{2m} \right) \psi(x, \mathbf{K}, E) + V_0(x)\psi(x, \mathbf{K}, E) \\ & - \frac{e}{2} \int \frac{\mathrm{d}\mathbf{K}'}{(2\pi)^2} \int_{-\infty}^{\infty} \frac{\mathrm{d}E'}{2\pi\hbar} \Phi_1(x, \mathbf{K} - \mathbf{K}', E - E')\psi(x, \mathbf{K}', E') \\ & - \frac{e}{2} \int \frac{\mathrm{d}\mathbf{K}'}{(2\pi)^2} \tilde{\Phi}_2(x, \mathbf{K} - \mathbf{K}', E)\psi(x, \mathbf{K}', E). \end{aligned} \tag{12}$$

Here $\tilde{\Phi}_2(x, \mathbf{K}, E)$ differs from $\Phi_1(x, \mathbf{K}, E)$ by being a one-sided Fourier or Laplace transform thus:

$$\tilde{\Phi}_2(x, \mathbf{K}, E) = \int_0^{\infty} \mathrm{d}t\, \mathrm{e}^{\mathrm{i}Et/\hbar} \Phi_2(x, \mathbf{K}, t). \tag{13}$$

Then the reality of the image potential $\Phi_1(x, \mathbf{R}, t)$, see equation (7), requires that the generally complex function $\Phi_1(x, \mathbf{K}, E)$ satisfy the symmetry:

$$\Phi_1^*(x, \mathbf{K}, E) = \Phi_1(x, -\mathbf{K}, -E), \tag{14}$$

whereas no such symmetry exists for the generally complex function $\tilde{\Phi}_2(x, \mathbf{K}, E)$. However, the latter has various analyticity properties for the continuation to the complex E plane as required by causality, namely the function $\tilde{\Phi}_2(x, \mathbf{K}, E)$ is only analytic in the whole upper E plane with a branch cut on the real axis, below which it can have singularities [11]. This property is *not* shared by $\Phi_1(x, \mathbf{K}, E)$ on the other hand, which can have singularities anywhere in the complex E plane, except at the origin. However, one must note that the physical input particle energy E as well as the final particle energy E_f as measured at the detector must both be real. Therefore, as mentioned before, any approximate many-body derivation of the image potentials should in principle preserve the above symmetry and analyticity properties. The analogous relation to equation (9) in energy space can also be derived from the definition of the Fourier transforms which leads to the convolution property:

$$\int_{-\infty}^{\infty} \mathrm{d}E'\, \psi(\mathbf{r}, -E + E')\psi^*(\mathbf{r}, E')\tilde{\Phi}_2^*(\mathbf{r}, E') = \int_{-\infty}^{\infty} \mathrm{d}E'\, \psi^*(\mathbf{r}, E + E')\psi(\mathbf{r}, E')\tilde{\Phi}_2(\mathbf{r}, E'). \tag{15}$$

In deriving the above result, the energy integration contours are closed in the upper-half plane in an anti-clockwise manner for the RHS of equation (15) (and in the lower-half plane in a clockwise manner for the LHS), as required by the analyticity property of $\tilde{\Phi}_2(x, \mathbf{K}, E)$ discussed above. Note that, for real $\Phi_2^*(\mathbf{r}, t)$, equation (9) can only be satisfied for real wavefunctions $\psi(\mathbf{r}, t)$ and accordingly equation (15) with wavefunctions of the symmetry equation (14), i.e. for stationary states. We shall later utilize the concept of quasi-stationary states in order to make further progress.

[2] Unless otherwise stated to avoid ambiguity, we shall use the usual physicist's notation for Fourier transform pairs through their arguments and reserve the tilde for later use to denote a one-sided transform.

2.2. Elastic and inelastic scattering

One final important observation before continuing is to note that the third term in equation (12), which contains the energy convolution $\Phi_1(x, \mathbf{K}, E - E')$, is the only term in the Schrödinger equation that leads to inelastic scattering for $E \neq E'$. As a result the Schrödinger equation in energy space couples to all available energy states and in particular leads to real excitations of the various modes that are accessible to the tunnelling electron as mentioned earlier. However, so long as the unitary conditions are satisfied, it can be shown that the tunnelling current is given by the usual expression:

$$\mathbf{J}(\mathbf{r}, t) = -\frac{\mathrm{i}e\hbar}{2m}\big(\psi^*(\mathbf{r}, t)\nabla\psi(\mathbf{r}, t) - [\nabla\psi^*(\mathbf{r}, t)]\psi(\mathbf{r}, t)\big), \tag{16}$$

that does not explicitly contain the interaction terms. Otherwise this formula is invalid and its use would lead to errors as mentioned earlier. The proof of the above theorem though lengthy follows the same essential steps as standard texts [16]. Without it, the usual wavefunction matching technique for the determination of the current through the transmission or reflection coefficients becomes inoperative. Note also that the unitarity condition equation (15) in energy space has features that are similar to the inelastic terms in the Schrödinger equation. This implies a close coupling between unitarity and inelastic scattering not present in ordinary time-dependent tunnelling processes that are not history dependent [17]. History dependence in the dynamical image problem appears to have been first brought to light in the early works of Mills [15]. In addition there are self-consistency issues, since the source of the potentials is due to the tunnelling particle itself; see later. Together these extraordinary features make the quantum tunnelling of a surface electron one of the most challenging problems in theoretical physics.

3. Working approximations

At this stage we shall, with some justification that has to be verified post hoc, ignore the inelastic terms. For the tunnelling systems we shall consider, the energy loss is assumed to be very small, and tunnelling is assumed to occur over a very narrow energy range, so that $\Phi_1(x, \mathbf{K}, E - E')$ is sharply peaked about $E' = E$. In this case the energy states are quasi-stationary. One can include a small imaginary lifetime to account for some energy loss. This is a quasi-particle description. The theory is then expected to be accurate only if this loss is small in some sense. One criterion is that this loss must be small compared to the total work done by the electron in being moved from the surface to the detector. According to recent studies, for sufficiently fast electrons, the total work done can be computed within the framework of classical electrodynamics [10, 12–14]. For slow electrons as in field emission the situation is not so clear. Indeed it is to be expected that near to the field emission threshold (where $F = F_c \approx 1$ V $\mu\mathrm{m}^{-1}$ for the carbon graphite systems) the energy losses will have a larger influence. As such, an accurate study of the threshold behaviour may require extensions beyond the present work.

3.1. Basic equations

Within the quasi-stationary approximation we derive the Schrödinger equation in energy space which forms the basis of our work throughout this paper:

$$E\psi(x, \mathbf{K}, E) = \left(-\frac{\hbar^2}{2m}\frac{\partial^2}{\partial x^2} + \frac{\hbar^2 K^2}{2m}\right)\psi(x, \mathbf{K}, E) + V_0(x)\psi(x, \mathbf{K}, E) - \frac{e}{2}\int \frac{\mathrm{d}\mathbf{K}'}{(2\pi)^2}\tilde{\Phi}_{\mathrm{I}}^{>}(x, \mathbf{K} - \mathbf{K}', E)\psi(x, \mathbf{K}', E), \tag{17}$$

where the image potential $\tilde{\Phi}_{\mathrm{I}}^{>}$ now absorbs all the energy diagonal terms and with the wavefunctions in real space and time being real, ignoring the small exponentially decaying parts as required by the quasi-stationary description. In view of the reality of all functions in real space and time, all complex quantities in energy momentum space, especially equation (17), must satisfy the symmetry property equation (14), which implies that all real parts are even functions of energy while imaginary parts are odd. Equation (17) makes contact with earlier workers dating back to Jonson [8]. Jonson and other later workers [18–20] used approximate self-energies which do not satisfy the above symmetry property equation (14). Therefore their theories cannot be accurate for the calculation of the tunnelling current in view of the unitarity issues discussed above, even though the real part of the resultant complex image potential they derive reduces to the classical image form in the appropriate limit. In view of the recently reported successful energy loss measurements due to image interaction in the photoemission of copper, our studies should motivate a careful re-examination of some of the above issues [21]. However, we shall not tackle these fundamental problems in the present work. Instead we shall accept the quasi-stationary approach, which in turn justifies a classical electrodynamic description of the image potential $\tilde{\Phi}_{\mathrm{I}}^{>}(\mathbf{r}, t)$ which we shall treat in the usual way. We remind the reader that this is not a proof but a working hypothesis. Indeed it is clear that a canonical quantization of the theory thus presented will not produce the full many-body quantum features inherent in the problem. In particular it cannot be justified by showing that the image potential reduces to the classical value alone. Its usefulness can only be judged by its agreement with experiments and whereupon it should motivate further deeper analysis of the quantum features.

Thus we start with a Poisson equation for the image field, assuming that the electron is emitted at time $t = 0$:

$$\nabla^2 \Phi^{>}(\mathbf{r}, t) = \frac{e}{\varepsilon_0} |\psi(\mathbf{r}, t)|^2 \qquad \text{for } x > 0 \tag{18}$$

$$\nabla \cdot [\hat{\mathcal{E}} \nabla' \Phi^{<}(\mathbf{r}', t')] = 0 \qquad \text{for } x < 0, \tag{19}$$

where $\Phi^{>} = \Phi_0^{>} + \Phi_{\mathrm{I}}^{>}$ and $\Phi^{<} = \Phi_0^{<} + \Phi_{\mathrm{I}}^{<}$ define the classical image potentials with Φ_0 representing the bare Laplace potential, which satisfies $\nabla^2 \Phi_0 = 0$. We have now removed the tilde on all the potentials since from what was said above their connection with the quantum self-energies is no longer straightforward, i.e. we equate $\tilde{\Phi}_{\mathrm{I}}^{>}$ with $\Phi_{\mathrm{I}}^{>}$ by hypothesis. The operator $\hat{\mathcal{E}}$ is the generally space time dispersive permittivity integral operator [22]:

$$\hat{\mathcal{E}} f(\mathbf{r}', t') = \int \mathrm{d}\mathbf{r}' \int_{-\infty}^{t} \mathrm{d}t' \, \varepsilon(\mathbf{r}, \mathbf{r}', t - t') f(\mathbf{r}', t'), \tag{20}$$

acting on an arbitrary *real* function f. Equations (18)–(20) formally complete the definition of the tunnelling problem posed by equations (2), with the dielectric function as external input.

3.2. Underlying limitations

At this stage we pause to consider a few limitations that are already apparent in this approach. First, the theory is only as good as the input dielectric function. Early work has shown that, for metals, with plasmon frequencies of order $f \sim 10^6$ GHz, quantum corrections due to electron–surface plasmon interactions become operative at $x_{\mathrm{s}} = (\hbar/(2m\omega_{\mathrm{s}}))^{1/2} \sim 1$ Å [23]. Second, the semi-classical treatment of the electromagnetic field fails if the field strength is too weak. The fundamental criterion is set by quantum electrodynamics which determines a distance $x_{\mathrm{QED}} = 4.35 \times 10^8 / f_{\mathrm{s}}$ nm GHz^{-1} $\sim$ 435 nm [24] where quantum corrections are unavoidable. These distances (see table 1) set the scale for the appropriate information that the semi-classical dielectric function must contain in order to provide an accurate description of the image potentials and therefore tunnelling. Fortunately, for lower plasmon frequencies,

Table 1. Estimated distance range from the surface where quantum corrections become significant. For $x < x_s$, quantum corrections are due to electron–surface plasmon interactions; for $x > x_{QED}$, quantum corrections are due to quantum electrodynamics.

f (Hz)	x_s (nm)	x_{QED} (nm)
10^{16}	0.0306	43.5
10^{15}	0.097	435
10^{14}	0.306	4350
10^{13}	0.970	4.35×10^4
10^{12}	3.06	4.35×10^5

the latter criterion for x_Q is more relaxed and becomes irrelevant. This is in agreement with the insignificance of retardation corrections to the image $1/x$ potential in contrast to the Casimir–Polder case [15, 25]. Unfortunately, the former criterion for x_s does not diminish in significance, for $f \sim 10^3$ GHz, $x_s \sim 3.06$ nm while $x_{QED} \sim 4.35 \times 10^5$ nm. However, the x_s values seem unreasonable at both ends of the frequency scale, and this is probably due to the simplicity of the model [23]. In fact we shall identify x_s with x_0 of our earlier work (see equation (41) of [1]) since in a more sophisticated model this is the distance where the electron–surface plasmon interactions start to modify the $1/x$ potential. Fortunately again, for tunnelling rates and especially for an enhanced potential, it is the wavefunction in the asymptotic (large x) region that determines the tunnelling probability, as we have seen in [1] and above. The close region is responsible for inelastic losses, which our theory can poorly describe at this stage. In the case of strong non-linear coupling, a single-valued externally input dielectric function, such as the bulk dielectric function as commonly used in linear response–surface plasmon theory, is unlikely to be adequate. This is where most of our work must first be focused. Even without considering this problem, equation (17) and equations (18)–(20) form a formidable self-consistent set at this level for the current source depends on the electron wavefunction as mentioned. An approximation using the classical point particle approach is close to being poor. For field emission the emitted particles have de Broglie wavelengths of the order of ∼10 Å (KE < 0.25 eV), whereas for EELs and for photo-emission these are of order <2.5 Å (KE > 5 eV) or less. The former is comparable to the width of the tunnelling surface region and thus the point charge model is close to its limit of validity. As we shall see below, there are non-linear susceptibility effects that come into play as well which we will need to consider for the carbon–graphite systems. Self-consistency of the dielectric function for strong non-linear coupling will then also become an issue that we will discuss later.

Before doing so we shall first recover the usual results from equation (17) by employing the point particle and slow particle approximations as well as a specular scattering assumption. The latter assumes that the magnitude of **K** remains constant during the tunnelling process. Since E is constant for quasi-stationary states then this means in particular that the x-component energy W (see [1] equation (13)):

$$W = E - \frac{\hbar^2 K^2}{2m}, \tag{21}$$

remains constant. This implies that the main scattering events are defined by the edges of the specular cone, where incident and scattered particles make the same angles with the x-axis; see figure 1. Furthermore, if the charge density of the tunnelling electron is spherically symmetric (as it will be for the point particle limit) and the dielectric function has azimuthal symmetry about the x-axis, then all functions of **K** can be replaced by their moduli. In particular, with specular scattering the wavefunction satisfies

$$\psi(x, \mathbf{K} - \mathbf{Q}, E) = \psi(x, |\mathbf{K} - \mathbf{Q}|, E) = \psi(x, |\mathbf{K}|, E) = \psi(x, K). \tag{22}$$

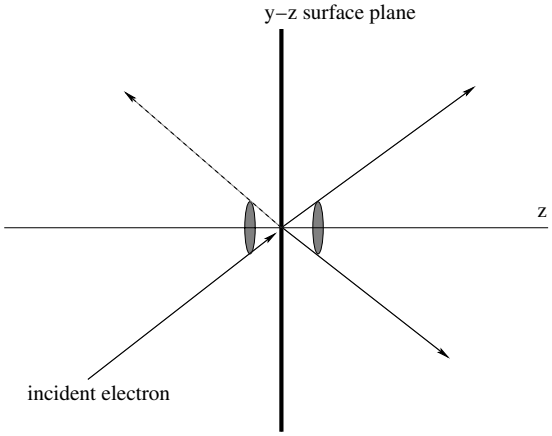

Figure 1. This figure illustrates the main specular scattering assumption in field emission where an incident electron is scattered by the surface plane (y–z) shown bold. In the quasi-stationary approximation these are the main events since E is constant, in which case so is the magnitude of $\mathbf{K}$ and thus the incident and scattered angles with the x-axis are identical. The scattered events are thus defined by the edge of specular cones (shaded), one for transmission and one for reflection. The dashed line shows the main specular reflection events central to surface plasmon theory [26, 28]. Note that for off-specular scattering, even with constant E, the magnitude K and therefore also the energy W (see equation (21)) are no longer conserved, in which case one has to revert to equation (17).

In this case, the Schrödinger equation (17) simplifies to:

$$E\psi(x, K, E) = \left(-\frac{\hbar^2}{2m}\frac{\partial^2}{\partial x^2} + \frac{\hbar^2 K^2}{2m}\right)\psi(x, K, E) + V_0(x)\psi(x, K, E) - \frac{e}{4\pi\varepsilon_0}\psi(x, K, E)\int_0^\infty Q\,\mathrm{d}Q\,\Phi_{\mathrm{I}}^{>}(x, Q, E). \tag{23}$$

An evaluation of the integral using the static dielectric function for a metal returns the classical image term: $-e^2/(16\pi\varepsilon_0 x)$, which forms the basis for the traditional Fowler–Nordheim theory [2, 3]. We will not reproduce this result here since it will follow in the course of our studies below. The reader should note that the above quasi-stationary and intrinsic specular scattering assumptions have been obscure in the history of field emission theory for the last 72 years and should now be included in updates of all modern texts, such as Modinos [27].

3.3. Key results

We shall retain specular scattering and allow for a charge distribution for the electron. For a dielectric, the induced potential can now be obtained by solving the appropriate boundary value problem [13, 26]. In this case the induced image potential can be written down as:

$$\Phi_{\mathrm{I}}^{>}(x, \mathbf{Q}, \omega) = \rho_{\omega\mathbf{Q}}\frac{\mathrm{e}^{-Qx}}{\kappa(\mathbf{Q}, \omega)}, \qquad \kappa(\mathbf{Q}, \omega) = \frac{\bar{\varepsilon}(\mathbf{Q}, \omega) + 1}{\bar{\varepsilon}(\mathbf{Q}, \omega) - 1}, \tag{24}$$

where we have absorbed ε_0 in the definition of $\bar{\varepsilon}$ (for convenience) which is now dimensionless, and also reverted to the usual frequency notation[3], where $\omega = (E + \mu)/\hbar$. Furthermore, we

[3] The reader should note that to relate this frequency scale to surface plasmons requires an order unity constant which for 3D plasmons has the form $\omega_{\mathrm{s}}/\mu = 0.6652\sqrt{r_{\mathrm{s}}/a_0}$. However, its accurate value is not straightforward (see remarks at the end of section 4).

have:

$$\rho_{\omega\mathbf{Q}} = \int_{-\infty}^{\infty} \mathrm{d}x \, \frac{\mathrm{e}^{-Q|x|}}{2Q} \rho(x, \mathbf{Q}, \omega); \tag{25}$$

in which $\rho(x, \mathbf{Q}, \omega)$ is the inverse partial Fourier transform of the probability density:

$$\rho(x, \mathbf{Q}, \omega) = \int \mathrm{d}\mathbf{R} \int_{-\infty}^{\infty} \mathrm{d}t \, \mathrm{e}^{\mathrm{i}\omega t} \mathrm{e}^{-\mathrm{i}\mathbf{Q}\cdot\mathbf{R}} |\psi(x, \mathbf{R}, t)|^2. \tag{26}$$

Equation (26) shows that for spherically symmetric charge distributions, $\rho_{\omega\mathbf{Q}} = \rho_{\omega|\mathbf{Q}|} = \rho_{\omega Q}$ is also spherically symmetric in K space. Further approximations are necessary to make progress, such as the static charge, in which $\rho_{\omega Q}$ is replaced by its static value ρ_{0Q}. We shall particularly be interested in the approximations that recover the classic Fowler–Nordheim case as a reference point before any more sophisticated work, and as we shall see, it is not the case of just a static charge.

Equation (24) contains the assumption of linear response and a quasi-classical bulk dielectric function $\varepsilon(\mathbf{q}, \omega)$ with $\mathbf{q} = (q, \mathbf{Q})$ for defining the averaged surface dielectric function $\bar{\varepsilon}(\mathbf{Q}, \omega)$:

$$\frac{1}{\bar{\varepsilon}(\mathbf{Q}, \omega)} = \frac{2}{\pi} \int_0^{\infty} \mathrm{d}q \, \frac{1}{\varepsilon(\mathbf{q}, \omega)} \frac{Q}{(Q^2 + q^2)}. \tag{27}$$

Equations (24)–(27) are highly non-trivial results. Equation (27) dates back to early surface plasmon theory [28]. In fact a more sophisticated average than equation (27) is also available within RPA theory involving the full off-diagonal dielectric matrix $\mathcal{E}(q, q', \mathbf{Q})$ due to the early works of Newns [29]. The latter will be important when off-specular scattering is considered even within the present quasi-stationary approach. The derivations simplify considerably if the spatial dispersion in the bulk dielectric function can be neglected, i.e. $\varepsilon(\mathbf{q}, \omega) \approx \varepsilon(\omega)$, in which case the Q dependence drops out of our previously defined κ function equation (24); see also equations (48) and (49) of [1]. However, we shall include anisotropy, which is likely to be important for systems such as CNTs. In this case the generalization is straightforward; see for example Mele [30].

$$\kappa(\omega) = \frac{\sqrt{\bar{\varepsilon}_x(\omega)\bar{\varepsilon}_r(\omega)} + 1}{\sqrt{\bar{\varepsilon}_x(\omega)\bar{\varepsilon}_r(\omega)} - 1}. \tag{28}$$

In equation (28) we have allowed for the anisotropy in the dielectric functions by assuming only two non-vanishing principal diagonal components for the permittivity tensor: $\mathcal{E} = (\varepsilon_x, \varepsilon_r, \varepsilon_r)$. Spatial dispersion can be ignored to a certain extent if the wavelengths of electromagnetic fluctuations are much larger than the spatial region under consideration. We shall do so from now on for convenience, but this should not be taken as obvious, especially when we need to consider the non-linear susceptibility terms. For now, we remark that it is the vanishing of $\kappa(\omega)$ close to the surface resonant mode ω_{s} that gives the potential enhancement which stimulates tunnelling. This is an image-induced resonant tunnelling phenomenon that seems to be unique to carbon–graphite systems. The above mathematical results provide a more quantitative statement of the discussions presented earlier in [1].

3.4. The limit of no spatial dispersion

We now specialize to the case in which spatial dispersion in $\kappa(\omega)$ can be neglected, as well as spherically symmetric s-state wavefunctions only. Then the integral in equation (23) is

$$\int_0^{\infty} Q \, \mathrm{d}Q \, \Phi_{\mathrm{I}}^{>}(x, Q, E) = \int_{-\infty}^{\infty} \mathrm{d}t \, \mathrm{e}^{\mathrm{i}\omega t} \int_0^{\infty} 2\pi R \, \mathrm{d}R \int_{-\infty}^{\infty} \mathrm{d}x' \, \frac{|\psi(\sqrt{x'^2 + R^2}, t)|^2}{2\kappa(\omega)\sqrt{(x + |x'|)^2 + R^2}}. \tag{29}$$

As discussed earlier, various approximations are necessary to make progress. We will not be able to examine all of these in this work but shall merely focus on the (a) point-particle and (b) instantaneous-tunnelling approximation which consists of

$$2\pi R|\psi(\sqrt{x'^2+R^2},t)|^2 = \delta(x'-x)\delta(R)\delta(t-t_0), \tag{30}$$

where t_0 is the notorious tunnelling transit time, which is a subject of some contention for the last decade [31]. Using the approximation equation (30), then equation (29) becomes:

$$\int_0^\infty Q\,\mathrm{d}Q\,\Phi_{\mathrm{I}}^{>}(x,Q,E) = \frac{\mathrm{e}^{\mathrm{i}\omega t_0}}{4x\kappa(\omega)} \approx \frac{1}{4x\kappa(\omega)}, \tag{31}$$

where the last step invokes the instantaneous-tunnelling approximation, whereby $\omega t_0 \ll 1$ is assumed. Note that this approximation violates the uncertainty principle, indicating that quantum processes *during* tunnelling have been ignored. The latter is nevertheless consistent with our quasi-stationary approximation. The further substitution of $\kappa(\omega) = \kappa(0)$, i.e. the static susceptibility, constitutes the Fowler–Nordheim approximation. Without digressing further we note in passing that other approximations are possible and remain to be studied in detail, such as the fast particle, instantaneous-tunnelling approximation, in which [13]:

$$2\pi R|\psi(\sqrt{x'^2+R^2},t)|^2 = \delta(x'-v_{\mathrm{F}}t)\delta(R)\Theta(t-t_0). \tag{32}$$

Instantaneous tunnelling is another intrinsic assumption of Fowler–Nordheim theory which we have adopted as well, but without the static κ assumption. It clarifies intuitive arguments of Sze [32] and used by us [1], which suggests that our earlier 3000 Å estimate is grossly underestimated. At this stage we have essentially recovered all our previous results in [1], in terms of the Nordheim–MacColl tunnelling model, except for the field dependence. Before we address the issue of the field dependence of the tunnelling, let us summarize the main results obtained thus far.

3.5. Interim summary

The approximations are (a) quasi-stationary states, (b) specular scattering, (c) instantaneous-tunnelling, and (d) point particle. In this case equation (23) now takes the form (see also equation (27) of [1]):

$$E\psi = \left(-\frac{\hbar^2}{2m}\frac{\partial^2}{\partial x^2} + \frac{\hbar^2K^2}{2m} + V_0(x) - \frac{e^2}{16\pi\varepsilon_0\kappa(\omega)x}\right)\psi, \tag{33}$$

where again $\omega = (E+\mu)/\hbar$ and we have now suppressed the arguments of $\psi = \psi(x, K, E)$ for convenience. Theoretically, when the electron energy E hits the surface plasmon resonance, $\omega = \omega_{\mathrm{s}}$, where $\kappa(\omega_{\mathrm{s}}) = 0$ or alternatively $\bar{\varepsilon}(\omega_{\mathrm{s}}) = \sqrt{\bar{\varepsilon}_x(\omega_{\mathrm{s}})\bar{\varepsilon}_r(\omega_{\mathrm{s}})} = -1$, then resonance tunnelling occurs and the image term dominates. We assume this is what happens in carbon–graphite field emitters. This was the scenario proposed in [1] in which the tunnelling current has already been calculated in the point particle approximation. Thus we have established the first criterion which appears to be fulfilled by carbon–graphite systems that makes enhanced field emission possible, that is their nano-structure enables a Fermi-energy level that is very close to the surface-plasmon resonant mode ω_{s}. This criterion alone is not sufficient though. For the proximity of the Fermi level to ω_{s} is measured by a resonance width $\Delta\omega$ which in turn is characterized by an analogous Q factor: Q_{f} (see below). Thus in practice two related issues need to be addressed. We shall do this in the next section.

4. Resonance and damping

The resonance is damped in any realistic system and thus there is only a narrow energy range by which resonance tunnelling can occur—this is in fact related to the ϑ electron concept proposed in [1]. The damping must be slow enough, at least much slower than the tunnelling period, in order for the enhanced potential to be effective in stimulating tunnelling. The latter issue is a complicated one; it involves going beyond the instantaneous tunnelling approach and may also involve velocity dependence and possibly other quantum effects. Unfortunately not enough is known on this issue at this stage for us to provide any more illuminating answers. Hence, apart from directing the interested reader to some related works [15, 13, 33] (which are mostly classical in their treatment), we shall have to postpone this interesting question at present. Even at an elementary level, discrepancies between the standard text-book model of relaxation has been a subject of some contention [34, 35]. We shall assume that whatever extra conditions are imposed by the above factors, they are satisfied as long as the damping is slow enough, since the tunnelling time across a layer of a few angstroms is likely to be in the femtosecond range or less for $v_F \sim 10^7$ cm s^{-1}, as estimated earlier in [1]. In this case we can estimate the damping by the use of a Drude-type formula for the dielectric function, assuming an isotropic model $\bar{\varepsilon}_x = \bar{\varepsilon}_r$ for convenience:

$$\bar{\varepsilon}(\omega) = 1 - \frac{\omega_p^2}{\omega(\omega + i\Gamma)} \qquad \Gamma = 1/\tau, \tag{34}$$

where τ is the Drude relaxation time. From equation (33), the effective dynamical Schottky barrier can be easily shown to be (see also equation (8) of [1]):

$$\Delta\phi(\omega) = e\sqrt{\frac{eF}{4\pi\varepsilon_0\kappa(\omega)}} = \varphi\sqrt{\frac{F}{F_b\kappa(\omega)}} \qquad \text{(eV)}. \tag{35}$$

Here we have $F_b = 694\varphi^2$ eV^{-2} V μm^{-1} (see equation (9) of [1]) as before. In the quasi-stationary approximation, only the real part of $\kappa(\omega)$ is relevant to the tunnelling Hamiltonian. It is then straightforward to derive the criterion:

$$\mathrm{Re}\sqrt{\frac{F}{F_b\kappa(\omega)}} = \sqrt{\frac{F}{F_b}}\left[\left(\frac{\omega_s^2}{\Gamma^2 + 4(\Delta\omega)^2}\right)^{1/4}\left(\frac{\pm\Delta\omega}{\sqrt{\Gamma^2 + 4(\Delta\omega)^2}} + \frac{1}{2}\right)^{1/2}\right] \geqslant 1, \tag{36}$$

where $\Delta\omega$ is a resonance half-width at ω_s in which the latter is given by $\bar{\varepsilon}(\omega_s) = -1$. The limiting case of $2\Delta\omega \gg \Gamma$ is the important one, in which case $\Delta\omega > 0$ is required. Both inequalities imply that the resonance is asymmetrical and it occurs just below the Fermi level and not above, a result that was in fact used in our earlier work; see for example equation (43) and (44) in [1]. We can now define a relevant $Q_f = \frac{\omega_s}{2\Delta\omega}$ which must be high as to be expected at the initial threshold fields, which requires:

$$Q_f \geqslant F_b/F. \tag{37}$$

The above formula implies that $Q_f \geqslant 10^3$ for a work function of $\varphi = 2$ eV at an onset field $F = F_0 \approx 2.78$ V μm^{-1}. From the above results we obtain a limit on the relaxation time Γ^{-1} of about 2 ps or longer for plasmon frequencies of order 2×10^{14} Hz or 200 THz. In classical plasmon theory, this would correspond to an electron density of one or two electrons per nm^3, which can be expected from free electrons on the surface nanostructure. However, this estimate must be crude, in view of the highly non-linear and field-dependent nature of our problem (see also the extra ω_0 parameter to be introduced in section 5).

The opposite limiting case of $2\Delta\omega \ll \Gamma$ occurs for most metals in which $\Gamma^{-1} \leqslant 10^{-14}$ s, and plasmon frequencies are of order 10^{15} Hz or more, then the criterion equation (36) fails

and the resonance is too damped to be effective unless the field is increased by at least two orders of magnitude to $F_0 = 100\ \mathrm{V}\ \mu\mathrm{m}^{-1}$. However, at such large fields the field dependence of the damping factor Γ cannot be neglected (it is known to follow roughly an F^2 law), thereby making the criterion impossible to satisfy.

It is to be noted that the above discussions will not be able to provide very accurate estimates for the number of available electrons (dubbed ϑ electrons in [1]), which is highly dependent on the line shape of the resonance. The latter is dependent on a number of factors, including the non-linear susceptibility; see the following section. The reader might like to know that the value of $Q_\mathrm{f} \sim 10^3$ is not by any means exceptional in terms of modern electronics where quartz crystals of $Q_\mathrm{f} \geqslant 10^4$ are readily fabricated. Presumably once the various Q_f controlling parameters are identified with suitable models, there will be new opportunities for nano-engineering of the surfaces of these materials for various applications not necessarily connected with field emission. As with all resonance phenomena, the interplay between damping and resonance is crucial and must be better understood. An under-damped system would make tuning impossible while an over-damped system will not resonate. For this reason we are motivated to move forward with further investigations of some preliminary models.

5. Non-linear susceptibility

We now show that we can obtain essentially the same results directly by considering the non-linear susceptibility. This reinforces the intuitive ideas of [1]. For in the limiting case where $2\Delta\omega \gg \Gamma$, i.e. when collision relaxation processes are no longer dominant, the non-linear second-order or higher-order electromagnetic processes come into play. Owing to the loss of inversion symmetry, the first non-linear term in the permittivity is indeed the quadratic term as mentioned in [1]. We express this in the standard form [37, 38]:

$$D_i(\omega = \omega_1 + \omega_2) = \varepsilon_{ij}(\omega)E_j(\omega) + \gamma_{ijk}(\omega_1, \omega_2)E_j(\omega_1)E_k(\omega_2), \tag{38}$$

where we have ignored spatial dispersion. The third rank tensor $\gamma_{ijk}(\omega, \omega')$ provides harmonic mixing and hence the optical rectification which has recently been observed to be anomalously large in carbon–graphite systems [36]. The inclusion of $\gamma_{ijk}(\omega, \omega')$ in equation (19) couples the dynamic field with the static field $\omega' = 0$. This is because field penetration is unavoidable in any realistic model. Indeed early calculations using an electron gas slab show that any external source field penetrates the surface to a depth of order $d = k_F^{-1}$ with an initial linear fall in the potential followed by an exponential tail with the classic Friedel oscillations [29]. For a dielectric we shall adopt a simpler linear field model to a depth of $d = k_F^{-1} \sim 7$ Å which is adequate for our purpose. Note that its value $eFd \sim 10^{-2}$ eV has little effect on the work function φ, whose value is 2 eV or more. Its main effect is to create a dynamical surface charge density that couples both dynamic and static fields at the interface. By including the second-order susceptibility as defined by equation (38), and after some lengthy calculations which we shall omit here, equation (19) in our partial Fourier space is now modified to:

$$\left[\left(\bar{\varepsilon}_x(\omega) + 2\frac{\gamma(\omega)}{\bar{\varepsilon}_{x0}}F\right)\frac{\partial^2}{\partial x^2} - \bar{\varepsilon}_r(\omega)K^2\right]\Phi^<(x, \mathbf{K}, \omega) = -2\frac{\gamma(\omega)}{\bar{\varepsilon}_{x0}}F\delta(x)\frac{\partial\Phi^<(x, \mathbf{K}, \omega)}{\partial x}, \tag{39}$$

where $\bar{\varepsilon}_{x0} = \lim_{\omega\to 0}\bar{\varepsilon}_x(\omega)$ is the static x-component of the dielectric constant. Here we have assumed that only a single non-vanishing component of the non-linear third rank permittivity tensor dominates, namely $\gamma_{xxx}(\omega, \omega') = \gamma(\omega)$, with all other components vanishing. This assumption can be justified by the fact that the other diagonal components, namely $\gamma_{yyy}(\omega, \omega')$ and $\gamma_{zzz}(\omega, \omega')$, vanish by symmetry, whereas off-diagonal components lead to higher-order K dependence that cannot be considered in isolation from spatial dispersion. Equation (39)

must be supplemented with appropriate boundary conditions that require the continuity of Φ and D_x, where the latter now takes the form:

$$\left(\bar{\varepsilon}_x(\omega) + 2\frac{\gamma(\omega)}{\bar{\varepsilon}_{x0}}F\right)\frac{\partial}{\partial x}\Phi^<(x, \mathbf{K}, \omega)_{x=0} = \frac{\partial}{\partial x}\Phi^>(x, \mathbf{K}, \omega)_{x=0}. \tag{40}$$

For zero non-linearity ($\gamma(\omega) = 0$), the problem reduces to the linear case as required. It is here that carbon–graphite systems differ from conventional metals, where evidence for anomalously large values of non-linear coefficients have been reported [36]. The effect of a finite $\gamma(\omega)$ is to modify equation (28) to the form:

$$\kappa(\omega) = \frac{(\bar{\varepsilon}_r(\omega)\alpha_F(\omega))^{1/2} + 1}{(\bar{\varepsilon}_r(\omega)\alpha_F(\omega))^{1/2} - 1}, \qquad \alpha_F(\omega) = \bar{\varepsilon}_x(\omega) + 2\frac{\gamma(\omega)}{\bar{\varepsilon}_{x0}}F. \tag{41}$$

Equation (41) underscores the non-linear dynamical image enhancement that sets apart the carbon–graphite systems. As before this can be analysed in the context of the Drude model equation (34). We will only study this at the peak of the resonance here, since we do not have a model for $\gamma(\omega)$ at this stage (see the next section), which in the relevant limit $1 \gg \gamma(\omega_s)F \gg 2\Gamma/\omega_s$ shows that the enhancement factor

$$\frac{1}{\kappa(\omega_s)} \sim 1 - \frac{2}{\gamma(\omega_s)F} + 4\mathrm{i}\frac{\Gamma}{\omega_s\gamma(\omega_s)^2F^2}. \tag{42}$$

Here we have again used the Drude model for $\bar{\varepsilon}(\omega)$, specializing to the isotropic case for convenience. Once again only the real part is relevant for the quasi-stationary approximation while the imaginary part is vanishingly small in the limit $\gamma(\omega_s)F \gg 2\Gamma/\omega_s$ in any case. Comparing the second term to the results of the previous section we now have the important relation:

$$|\gamma(\omega_s)| \geqslant 2/F_b, \qquad (\mathrm{V}/\mu\mathrm{m})^{-1} \tag{43}$$

which replaces the previous criterion equation (36) at resonance. Note again that in the limit discussed, i.e. when collision times are not dominant, the criterion and equation (42) require that $\gamma(\omega_s)$ must be negative. Its interpretation will be shown in the next section. We should remark that such a non-linear property may not be able to exist in isolation. Indeed if the coupling becomes large, the choice of an external input dielectric function even with optical non-linearity included needs to be re-examined from the point of view of self-consistency. Before doing so we should investigate by the use of a simple microscopic model how our various parameters (in particular γ) can be related to microscopic parameters.

6. Non-linear susceptibilities and the Duffing oscillator model

The subject of non-linear susceptibilities is often treated by the use of simple text-book type models. This is in fact a useful approach before considering any detailed microscopic quantum models, since many of the features due to non-linear behaviour at the classical level can already be captured by such models. Indeed considerable advantages can be gained by doing so, since many interesting features peculiar to non-linear systems, such as limit cycles, bifurcation, period doubling and chaos, are nowadays understood to contain universal features that can be treated by renormalization group theory. The well known driven Duffing oscillator is a case in point:

$$\ddot{x} + \Gamma\dot{x} + \omega_0^2 x + ax^2 + bx^3 = \frac{e}{m}\mathcal{F}. \tag{44}$$

We shall consider N such independent oscillators as a model for the surface plasmon modes and without loss of generality confine our discussions to the one-dimensional case for the

moment. To simplify the algebra further we shall ignore the quartic anharmonicity term and retain the cubic term only, since a stability analysis of the solutions is not our objective at this stage. By considering the driven field to contain two Fourier components only, i.e.

$$\mathcal{F} = E_1 \mathrm{e}^{-\mathrm{i}\omega_1 t} + E_2 \mathrm{e}^{-\mathrm{i}\omega_2 t} + \text{c.c.}, \tag{45}$$

standard perturbation analysis can be used to expand the electric polarization in terms of the higher-order non-linear susceptibilities:

$$\begin{aligned} P(t) = Nex(t) = {} & \chi^{(1)}(\omega_1)E_1 + \chi^{(1)}(\omega_2)E_2 \\ & + \chi^{(2)}(\omega_1 \pm \omega_2)E_1E_2 + \chi^{(2)}(\omega_1)E_1^2 + \chi^{(2)}(\omega_2)E_2^2 \\ & + \chi_1^{(2)}(0)E_1^2 + \chi_2^{(2)}(0)E_2^2 + \text{c.c.}, \end{aligned} \tag{46}$$

where the last two terms are the well known optical rectification terms [36, 38, 39] and we have suppressed the time-dependent exponential factors for brevity. The result of such an analysis gives the following expressions for the various linear and non-linear susceptibilities as [39]:

$$\chi^{(1)}(\omega_\ell) = \frac{\omega_\mathrm{p}^2}{\omega_0^2 - \omega_\ell^2 - \mathrm{i}\omega_\ell\Gamma}, \qquad \omega_\mathrm{p}^2 = \frac{Ne^2}{\varepsilon_0 m} \qquad \text{for } \ell = 1, 2. \tag{47}$$

For $\omega_0 = 0$ (pure plasmon mode) the above yields the standard Drude formula equation (34), but as we shall see later ω_0 is finite and does have a significant role. We present the following non-linear susceptibility formulae, bearing in mind that we are only working to cubic non-linearity, i.e. $a \neq 0, b = 0$:

$$\chi^{(2)}(\omega_1 \pm \omega_2) = -\frac{2(ae/m)\omega_\mathrm{p}^2}{(\omega_0^2 - \omega_1^2 - \mathrm{i}\omega_1\Gamma)(\omega_0^2 - \omega_2^2 \mp \mathrm{i}\omega_2\Gamma)(\omega_0^2 - (\omega_1 \pm \omega_2)^2 + \mathrm{i}(\omega_1 \pm \omega_2)\Gamma)}. \tag{48}$$

This is the sub-harmonic mixing term which is of most concern to us. We include the other terms for completeness, since they are known to be of significance in other areas outside field emission:

$$\chi^{(2)}(2\omega_\ell) = -\frac{(ae/m)\omega_\mathrm{p}^2}{(\omega_0^2 - \omega_\ell^2 - \mathrm{i}\omega_\ell\Gamma)(\omega_0^2 - 4\omega_\ell^2 - \mathrm{i}2\omega_\ell\Gamma)} \qquad \text{for } \ell = 1, 2, \tag{49}$$

which is the second harmonic mixing term, and finally:

$$\chi_1^{(2)}(0) = -\frac{(ae/m)\omega_\mathrm{p}^2}{\omega_0^2(\omega_0^2 - \omega_1^2 - \mathrm{i}\omega_1\Gamma)}, \tag{50}$$

and

$$\chi_2^{(2)}(0) = -\frac{(ae/m)\omega_\mathrm{p}^2}{\omega_0^2(\omega_0^2 - \omega_2^2 - \mathrm{i}\omega_2\Gamma)}, \tag{51}$$

are the optical rectification terms.

Now we come back to the matters at hand and concentrate on equations (47) and (48). Equation (47) shows that the surface plasmon resonance is affected by ω_0:

$$\omega_\mathrm{s}^2 = \omega_0^2 + \frac{\omega_\mathrm{p}^2}{2}, \tag{52}$$

whose origin lies outside classical plasmon theory. Equation (48) shows that the second-order non-linear coefficient $\gamma(\omega)$ defined in the previous section can be related to the cubic anharmonicity parameter a via

$$\gamma(\omega) = \lim_{\omega_2 \to 0} \chi^{(2)}(\omega \pm \omega_2) = -\frac{(2ae/m)\omega_\mathrm{p}^2}{\omega_0^2[(\omega_0^2 - \omega^2)^2 + \omega^2\Gamma^2]}. \tag{53}$$

Note that this quantity is real (hence its effect on the resonance is non-dissipative) and in the limit of $\omega_p \gg \omega_0$ and small damping $\omega_p \gg \Gamma$, reduces to the important result:

$$\gamma(\omega_s) = -\frac{2ae}{m\omega_0^2\omega_p^2}. \tag{54}$$

First of all, a negative value of $\gamma(\omega_s)$ at resonance (see previous section) implies a positive value of a i.e. a symmetrical hard spring ensues. For a negative a this would be an asymmetrical spring, soft for $x > 0$ and hard for $x < 0$, which is not our case. Second, note that our perturbation method fails in the limit $\omega_0 \to 0$, implying that it has a critical role to play. We are led therefore to conclude that the surface plasmon mode of relevance to our previous discussions is not a pure plasmon mode. We can estimate the ratio a/ω_0^2 from the value of F_b via equation (43) with the usual work function of 2 eV and a plasmon frequency of 10^{14} Hz. This gives $a/\omega_0^2 \approx 7.9 \times 10^6$ cm^{-1}, indicating that for nanometre size oscillations, the non-linear terms are already too large to justify a perturbation analysis. More sophisticated methods of non-linear analysis are available starting from standard textbook techniques [40]. However, this will not alter the general picture of the surface plasmon mode resonance and damping characteristics presented here except in detail, bearing in mind that neither periodic nor aperiodic solutions are of main interest to us, but rather the transient short time behaviour at resonance.

To conclude the present studies we must come back to the issue of the self-consistency of the dielectric function. The strong non-linear coupling indicated by the above studies requires that we must develop some method of assessing the significance of other underlying non-linear many-body effects that this study entails. This we shall do in the next section.

7. Dielectric function—self-consistency

Our main purpose here is to describe the underlying many-body physics. For clarity, we shall suppress all indices and arguments unless essential to avoid ambiguity. In section 2, we have highlighted the important role played by the exact single particle self-energies Σ of the tunnelling electron in determining the image potentials, and thus tunnelling probabilities. Bearing in mind that all our quantities are dependent on the applied external field F, these self-energies are in fact related to the dielectric function $\mathcal{E}$ via the many-body expression that is a generalization of the RPA result [41]:

$$\Sigma(k) = -\frac{1}{L^2 d}\sum_{\mathbf{q},\mathrm{i}q_n} \frac{\upsilon_q}{\beta}\frac{\mathcal{G}(k+q)}{\mathcal{E}(q)}, \qquad \beta = \frac{1}{k_B T}. \tag{55}$$

Here the sum is over all momentum $\mathbf{q}$ and Matsubara frequencies $\mathrm{i}q_n = \mathrm{i}(2n{+}1)\pi/\beta$, with k and q being symbolic four-dimensional quantities, L^2 being the planar area and d an appropriate slab width. The quantity υ_q is the appropriate Fourier component of the bare Coulomb potential while $\mathcal{G}$ is an appropriate single particle Green function, and for the first time in this paper we are bringing temperature into play. The appropriate Green function will be the non-interacting free particle Green function $\mathcal{G}^0$ in the case of an electron gas model but will be given by an appropriate Dyson equation if other degrees of freedom are involved, as the presence of a finite ω_0 in the last section seems to imply. If equation (55) were to be exact, not only must $\mathcal{G}$ be exact, but the exact dielectric function $\mathcal{E}$ must also be self-consistent with Σ, for conversely by inversion, equation (55) can also be used to obtain $\mathcal{E}$, if instead $\Sigma(k)$ were the given quantity. In view of the strong non-linear coupling discussed previously, some handle on this self-consistency issue is important. The reason is that *a priori* we do not know if this self-consistency correction to the externally input $\mathcal{E}$ that we have been using so far

(we emphasize that here we have included all non-linear field dependence in $\mathcal{E}$ as well) will lead to a stronger or a weaker non-linear field-dependent damping than the picosecond limit collision damping that we have been assuming so far. If it is the former then our present theory will be in trouble. If it is the case of a weaker non-linear field dependent damping, then there is compelling evidence that we have now essentially pinned down the major ingredients for a time-dependent field enhanced tunnelling theory for the carbon field emitters.

We begin by recalling that for a generally complex dielectric function at the resonant frequency ω_s, where

$$\frac{\varepsilon_s(\omega_s)}{\varepsilon_0} = -1 + i\tilde{\epsilon}_s, \qquad 0 < \tilde{\epsilon}_s \ll 1, \tag{56}$$

the enhancement factor κ_s^{-1} of the image potential is related to $\tilde{\epsilon}_s$ by:

$$\kappa_s^{-1} = \kappa(\omega_s)^{-1} \approx 1 + i\frac{2}{\tilde{\epsilon}_s}. \tag{57}$$

In the limit of small $\tilde{\epsilon}_s$, the dynamical Schottky barrier is determined by:

$$\mathrm{Re}\,\kappa_s{}^{-1/2} \to \tilde{\epsilon}_s^{-1/2}, \tag{58}$$

irrespective of the underlying origin of the complex term. We have learnt that the surface mode damping term at the resonant frequency given by $\tilde{\epsilon}_s$ actually determines the effectiveness of the potential enhancement, since an absolute zero value of $\tilde{\epsilon}_s$ is unrealistic, which would also imply a zero line width: an impossible tuning situation. It remains for us to examine the effect that further non-linear feedback due to the self-consistency in $\mathcal{E}$ has on the enhancement factor, as its effect is dissipative and potentially harmful. The approach is not to attempt to solve the problem from first principles. Rather we shall consider a one-dimensional fluctuating barrier model and focus on the relaxation time $\tau = \Gamma^{-1}$ which we shall relate to the above imaginary part $\tilde{\epsilon}_s$ by the same Drude relation: $\tilde{\epsilon}_s = 2\Gamma/\omega_s$; see equation (36). Note that this relaxation time neglects collision or correlation effects which we have previously identified as a prerequisite condition for enhanced tunnelling. This philosophy is inspired by related issues in the quantum theory of diffusion as applied to light interstitials in metals, developed more than thirty years ago by Flynn and Stoneham [42].

7.1. Fluctuating barrier model

In introducing the model we shall measure all energies with respect to the Fermi level as before. Then the time-dependent Schrödinger equation is given by:

$$i\hbar\frac{\partial\psi(x,t)}{\partial t} = -\frac{\hbar^2}{2m}\frac{\partial^2\psi(x,t)}{\partial x^2} + V_f(x,t)\psi(x,t). \tag{59}$$

Our simplified fluctuating barrier model is defined by the time-dependent confining potential $V_f(x,t)$:

$$V_f(x,t) = \begin{cases} -\mu & \text{for } x < 0\text{—region 1;} \\ \varphi - \Delta\phi(\omega)\Theta(t)\cos(\omega t) & \text{for } x > 0\text{—region 2,} \end{cases} \tag{60}$$

where $-\mu$ is the bottom of the band, φ is the work function, $\chi = \varphi + \mu$ is the electron affinity, $\omega = (E + \mu)/\hbar$ and $\Delta\phi(\omega)$ is given by equation (35). The latter mimics the fluctuating potential due to the dynamical Schottky image effect in an applied field and will be treated

as an impulse perturbation, consistent with instantaneous tunnelling, $\omega t_0 \ll 1$; see the end of section 3. In the absence of the perturbation, all the bound state wavefunctions are given by:

$$\psi_k(x) = \begin{cases} \dfrac{1}{\sqrt{L}} \sin(kx + \delta_0) & \text{for } x < 0\text{—region 1;} \\ \dfrac{1}{\sqrt{L}} \sin\delta_0 \mathrm{e}^{-\tilde{k}x} & \text{for } x > 0\text{—region 2,} \end{cases} \tag{61}$$

where:

$$k = \sqrt{\frac{2m}{\hbar^2}(E+\mu)} \qquad \text{and} \qquad \tilde{k} = \sqrt{\frac{2m}{\hbar^2}\chi - k^2}, \tag{62}$$

and the phase shift δ_0 is given by:

$$\tan\delta_0 = -\frac{k}{\tilde{k}} = -\sqrt{\frac{E+\mu}{\varphi - E}}. \tag{63}$$

The unbound state wavefunctions can also be written down, but they are of no relevance to us and we will not discuss these further here. For this simple model, the exact wavefunctions Ψ_k after the impulse are also known, by simply changing $\varphi \to \varphi - \Delta\phi(\omega)$. Hence, in principle, the exact transition probability in the impulse approximation can be calculated for this simple model [43]:

$$\tilde{\epsilon}_\mathrm{s} = \frac{2}{\omega_\mathrm{s}\tau} = 2\sum_{k_i,k_\mathrm{f}} \left| \int \mathrm{d}x\, \psi_{k_i} \Psi^*_{k_\mathrm{f}} \right|^2 f_{k_i}(1 - f_{k_\mathrm{f}}), \tag{64}$$

where now we merely focus on the peak $\omega = \omega_\mathrm{s}$, since off-peak contributions are of higher order and the Drude relation equation (36) has been assumed. The Fermi factors f_k are also included to ensure transitions only between occupied and empty states. However, a first-order perturbation calculation suffices, in which case the above expression becomes [43]:

$$\tilde{\epsilon}_\mathrm{s} = 2\sum_{k_i,k_\mathrm{f}} \frac{|\Delta\phi_{k_i,k_\mathrm{f}}|^2}{(E_{k_i} - E_{k_\mathrm{f}})^2} f_{k_i}(1 - f_{k_\mathrm{f}}), \tag{65}$$

where we have used a simplified notation in which $E_k = E(k)$ as given by inverting the first of equation (62). Note that this equation now gives a self-consistency relation, since $\Delta\phi_{k_i,k_\mathrm{f}}$ is itself dependent on $\tilde{\epsilon}_\mathrm{s}$ in our model. It is also important to note that for a higher-dimensional model, in doing the above sum over states, there will also be K dimensional constraints not present in one dimension. A straightforward evaluation of the matrix elements yields the result:

$$\Delta\phi_{k_i,k_\mathrm{f}} = \frac{1}{L}\Delta\phi(\omega_\mathrm{s}) \frac{\sin\delta_0(\tilde{k}_i)\sin\delta_0(\tilde{k}_\mathrm{f})}{\tilde{k}_i + \tilde{k}_\mathrm{f}}. \tag{66}$$

Using equations (35) and (58) we have the final result:

$$\tilde{\epsilon}_\mathrm{s}^2 = \frac{2\varphi^2 F}{L^2 F_\mathrm{b}} \sum_{k_i,k_\mathrm{f}} \frac{\sin^2\delta_0(\tilde{k}_i)\sin^2\delta_0(\tilde{k}_\mathrm{f})}{(E_{k_i} - E_{k_\mathrm{f}})^2(\tilde{k}_i + \tilde{k}_\mathrm{f})^2} f_{k_i}(1 - f_{k_\mathrm{f}}). \tag{67}$$

The sums are easily converted to integrals using the usual formulae:

$$\frac{1}{L}\sum_k \to \frac{1}{2\pi}\int \mathrm{d}k \to \frac{1}{2\pi\hbar}\sqrt{\frac{m}{2}}\int \frac{\mathrm{d}E}{\sqrt{\varphi - E}}. \tag{68}$$

Note that there can be no optical transitions (since there are no external energy sources and only the ϑ electrons are involved in the resonance), so that upon integrating over the ϑ electrons:

$$\tilde{\epsilon}_\mathrm{s}^2 = \frac{\varphi F}{32\pi^2 F_\mathrm{b}} \int_{-\vartheta}^{0-} \frac{\mathrm{d}E_i}{\sqrt{\varphi - E_i}} \int_{0+}^{\vartheta} \frac{\mathrm{d}E_\mathrm{f}}{\sqrt{\varphi - E_\mathrm{f}}} \frac{\sin^2\delta_0(E_i)\sin^2\delta_0(E_\mathrm{f})}{(E_i - E_\mathrm{f})^2}(f_{E_i} - f_{E_\mathrm{f}}). \tag{69}$$

Table 2. Damping time τ in picoseconds from equation (73) as a function of the work function φ (eV) and applied field F V μm^{-1}, with a plasma frequency $\omega_p = 4\pi \times 10^{14}$ Hz.

$F\|\varphi$	1	2	3	4	5
1	1.5806	3.1613	4.7419	6.3225	7.9032
5	0.7069	1.4138	2.1206	2.8275	3.5344
10	0.4998	0.9997	1.4995	1.9994	2.4992
15	0.4081	0.8162	1.2244	1.6325	2.0406
20	0.3534	0.7069	1.0603	1.4138	1.7672

For the small range of integration, we have from equation (62):

$$\tilde{k}_i + \tilde{k}_f \approx 2\sqrt{\frac{2m\varphi}{\hbar^2}}, \tag{70}$$

and further the difference of the Fermi factors over the energy range can be approximated by a delta function, so that

$$\frac{(f_{E_i} - f_{E_f})}{(E_i - E_f)^2} \to \frac{1}{\vartheta}\delta(E_i - E_f + \vartheta), \tag{71}$$

while the rest of the integrand changes little over the range of integration. We then arrive at:

$$\tilde{\epsilon}_s^2 = \frac{1}{32\pi^2}\frac{F}{F_b}\sin^4\delta_0(0) = \frac{1}{72\pi^2}\frac{F}{F_b}, \tag{72}$$

or alternatively:

$$\tilde{\epsilon}_s = \frac{2}{\omega_s\tau} = \frac{1}{6\pi}\sqrt{\frac{F}{2F_b}}, \tag{73}$$

which is a weaker damping law and hence not potentially destructive to the enhancement which goes as $\kappa_s^{-1} \sim (\gamma(\omega_s)F/2)^{-1}$ due to the non-linear susceptibility as found earlier. A numerical estimate for the relaxation time from the Drude relation $\omega_s\tau = 2/\tilde{\epsilon}_s$ gives $\tau \approx 1.9$ ps at the onset field, once again with the usual work function of 2 eV and a plasmon frequency of 2×10^{14} Hz, which is comparable to the neglected collision times. In table 2 we provide the damping times for various work functions and applied fields as calculated from equation (73), which are all in the range of picoseconds. Note that this (dissipative) feedback mechanism favours a larger work function, and although the relaxation times decrease slightly with a larger field, the required Q factor also diminishes as the field F increases according to a faster law, thus cancelling its negative effect; see equation (37). Higher-order corrections to the field dependence will need a more involved study, as mentioned also in our earlier work concerning the current [1].

We emphasize that there is no loss of generality in using a one-dimensional model here. The extension to higher dimensions within an RPA theory can be obtained by a similar generalization of the early work of Newns [29], but whose impenetrable barrier model must be suitably modified as above (see equation (61)). We leave open the question if these higher-dimensional models will lead to an even weaker power law, i.e. $\tilde{\epsilon}_s \sim F^{1/x}$ with $x > 2$, where simple phase space arguments suggest that this would be the case. We now turn to a re-examination of the tunnelling current in the present formalism. This will highlight important issues and provide contact with our earlier calculations [1].

8. Tunnelling current

In calculating the tunnelling current we return once again to the key formula given by equation (16), which as stated earlier is valid as long as the various unitarity and causality conditions are met. The alert reader will notice that the various wavefunctions and their derivatives have been written in a specified order for a very good reason. For the fermion system that satisfy Fermi–Dirac statistics (see assumption 1 in section 1 of our earlier paper [1]), equation (16) can be immediately transcribed in the second quantization formalism as the time-dependent current operator:

$$\hat{\mathbf{J}}(\mathbf{r},t) = -\frac{\mathrm{i}e\hbar}{2m}\big(\hat{\psi}^{\dagger}(\mathbf{r},t)\nabla\hat{\psi}(\mathbf{r},t) - [\nabla\hat{\psi}^{\dagger}(\mathbf{r},t)]\hat{\psi}(\mathbf{r},t)\big), \tag{74}$$

where now the order of the field operators $\hat{\psi}(\mathbf{r},t)$ and $\hat{\psi}^{\dagger}(\mathbf{r},t)$ is extremely important. In view of our partial Fourier transform definition equation (11), we can write these second quantized field operators as:

$$\hat{\psi}(x,\mathbf{R},t) = \sum_{\mathbf{K}}\int_{-\infty}^{\infty}\frac{\mathrm{d}E}{2\pi\hbar}\mathrm{e}^{-\mathrm{i}Et/\hbar}\mathrm{e}^{\mathrm{i}\mathbf{K}\cdot\mathbf{R}}\hat{C}_{\mathbf{K}E}\psi(x,\mathbf{K},E), \tag{75}$$

and its conjugate:

$$\hat{\psi}^{\dagger}(x,\mathbf{R},t) = \sum_{\mathbf{K}}\int_{-\infty}^{\infty}\frac{\mathrm{d}E}{2\pi\hbar}\mathrm{e}^{\mathrm{i}Et/\hbar}\mathrm{e}^{-\mathrm{i}\mathbf{K}\cdot\mathbf{R}}\hat{C}^{\dagger}_{\mathbf{K}E}\psi^{*}(x,\mathbf{K},E); \tag{76}$$

where $\hat{C}_{\mathbf{K}E}$ and $\hat{C}^{\dagger}_{\mathbf{K}E}$ are appropriate fermion operators and we have changed the integral over $\mathbf{K}$ to a sum for normalization reasons that will become clear later. Otherwise, the wavefunctions $\psi(x,\mathbf{K},E)$ satisfy the same Schrödinger equation as before, i.e. equation (12), where no approximations have yet been made. We now need to address two issues that are important for the calculation of the current. The first and more trivial issue is the appropriate normalization for the wavefunctions. Standard practice is to normalize the real space wavefunctions $\psi(x,\mathbf{R},t)$ to $L^{-3/2}$, with L a large linear dimension of space, since the integral over all space of $|\psi(x,\mathbf{R},t)|^2$, taking $L\to\infty$, is unity at *all* times. From this we can deduce that $\psi(x,\mathbf{K},E)$ is normalized to:

$$\psi(x,\mathbf{K},E) \sim \frac{1}{\sqrt{\upsilon}}\sqrt{\frac{\tau_0}{L^2}}, \tag{77}$$

where υ is the incident particle velocity and τ_0 is some macroscopic timescale which is of the order of seconds in our case. Both L and τ_0 are taken to infinity at the end of the calculations. The second harder issue concerns the appropriate anti-commutation relations for the fermion operators. Without invoking any approximations, all we can say is that, for a fixed energy E, the operators $\hat{C}_{\mathbf{K}E}$ and $\hat{C}^{\dagger}_{\mathbf{K}'E}$ anti-commute:

$$\{\hat{C}_{\mathbf{K}E},\hat{C}^{\dagger}_{\mathbf{K}'E}\} = \delta_{\mathbf{K},\mathbf{K}'}, \tag{78}$$

since wavefunctions of different energies E, E' are in general non-orthogonal. To resolve this difficulty would require us to consider double-time or double-energy Green functions. It poses interesting questions for the calculation of the time dependence of the current or alternatively its energy distribution, which we will not examine here at present [21]. Fortunately, in calculating the steady state current these issues do not matter, since then we can average over timescales that are macroscopic, i.e. of order τ_0, and quantities such as:

$$\frac{1}{\tau_0}\int \mathrm{d}t\;\hat{\psi}^{\dagger}(x,\mathbf{R},t)\nabla\hat{\psi}(x,\mathbf{R},t) \to \frac{1}{\tau_0}\int \mathrm{d}t\sum_{\mathbf{K},\mathbf{K}'}\int\frac{\mathrm{d}E}{2\pi\hbar}\int\frac{\mathrm{d}E'}{2\pi\hbar}$$
$$\times\,\mathrm{e}^{-\mathrm{i}(\mathbf{K}-\mathbf{K}')\cdot R}\mathrm{e}^{\mathrm{i}(E-E')t/\hbar}\hat{C}^{\dagger}_{\mathbf{K}E}\hat{C}_{\mathbf{K}'E'}\psi^{*}(x,\mathbf{K},E)\nabla\psi(x,\mathbf{K}',E'), \tag{79}$$

leads to an integral over a delta function in E, as a result of the time average. The thermodynamic averaged current $J = \langle J_x \rangle$ then leads to the formula:

$$J = -\frac{\mathrm{i}e}{4\pi m\tau_0}\int \mathrm{d}E \sum_{\mathbf{K}} \langle \hat{n}_{\mathbf{K}}(E)\rangle \left[\psi^*(x,\mathbf{K},E)\frac{\partial\psi(x,\mathbf{K},E)}{\partial x} - \frac{\partial\psi^*(x,\mathbf{K},E)}{\partial x}\psi(x,\mathbf{K},E)\right], \tag{80}$$

where $\langle \hat{n}_{\mathbf{K}}(E)\rangle = \langle \hat{C}^{\dagger}_{\mathbf{K}E}\hat{C}_{\mathbf{K}E}\rangle$ is an equilibrium distribution function, which requires knowledge of the above-mentioned Green functions. Now assumption 2 in section 1 of our earlier paper [1] ensures that the equilibrium distribution is undisturbed by the tunnelling electrons, in which case:

$$\langle \hat{n}_{\mathbf{K}}(E)\rangle = f_{\mathbf{K}}(E) = \frac{1}{\exp\left[\beta(W + \frac{\hbar^2K^2}{2m})\right] + 1}, \qquad \beta = \frac{1}{k_{\mathrm{B}}T}. \tag{81}$$

We now need the quasi-stationary assumption of section 3, by which the wavefunction on the left region of the barrier ($x < 0$) can then be written as:

$$\psi(x,\mathbf{K},E) = \frac{1}{\sqrt{\upsilon}}\sqrt{\frac{\tau_0}{L}}(\mathrm{e}^{\mathrm{i}kx} + r_{\mathbf{K}}(E)\mathrm{e}^{-\mathrm{i}kx}), \qquad k = \left(\frac{2m(W+\mu)}{\hbar^2}\right)^{1/2}, \tag{82}$$

where $r_{\mathbf{K}}(E)$ is the reflection amplitude; see also equation (19) of our earlier paper [1], but note here the $\mathbf{K}$ and the E (*not* W) dependence of the amplitudes. As we have normalized the wavefunctions according to equation (77), this gives:

$$-\mathrm{i}\left[\psi^*(x,\mathbf{K},E)\frac{\partial\psi(x,\mathbf{K},E)}{\partial x} - \frac{\partial\psi^*(x,\mathbf{K},E)}{\partial x}\psi(x,\mathbf{K},E)\right] = \frac{2k\tau_0}{\upsilon L^2}\mathcal{T}_{\mathbf{K}}(E) = \frac{4\pi m\tau_0}{h}\mathcal{T}_{\mathbf{K}}(E), \tag{83}$$

in which $\mathcal{T}_{\mathbf{K}}(E) = 1 - |r_{\mathbf{K}}(E)|^2$ is the transmission coefficient. The expression for the current within the quasi-stationary approximation is then:

$$J = e\int \frac{\mathrm{d}E}{L^2}\sum_{\mathbf{K}} f_{\mathbf{K}}(E)\mathcal{T}_{\mathbf{K}}(E), \tag{84}$$

where the sum and the integral cannot be separated without further assumptions. This requires the specular scattering assumption (see section 3) in which case the energy integral over $\mathrm{d}E$ can be replaced by $\mathrm{d}W$. Also, because $\mathcal{T}_{\mathbf{K}}(E) = \mathcal{T}(W)$ the expression becomes independent of $\mathbf{K}$ and the final expression for the current is:

$$J = e\int \mathrm{d}W\, N(W)\mathcal{T}(W), \tag{85}$$

where:

$$N(W) = \frac{4\pi mk_{\mathrm{B}}T}{h^3}\ln\left\{1 + \exp\left[-\left(\frac{W}{k_{\mathrm{B}}T}\right)\right]\right\}, \tag{86}$$

is the well known supply function; see also equation (6) of our earlier paper [1]. This expression forms the basis of our earlier work and indeed a lot of other works on field emission, but the above should clarify the various underlying approximations that have to be invoked to get there. At this stage we need not repeated all our earlier calculations [1], except to highlight a few key steps made on the basis of earlier intuitions, which can now be substantiated by what we have learnt here. First the parameter x_0 (see equation (42) of [1]) can now be related to x_{s} in table 1, which effectively fixes the Q factor in a semi-empirical way. This assumption is now entirely reasonable since the neglect of inelastic processes during tunnelling (and hence the

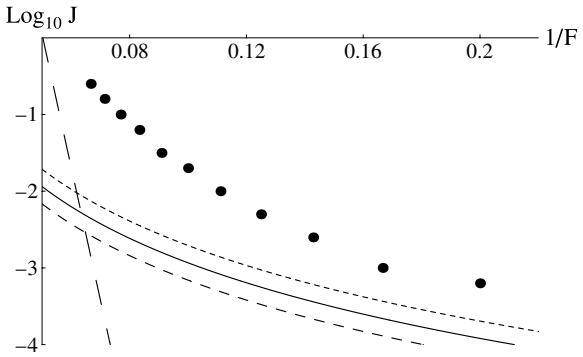

Figure 2. Logarithmic $\log_{10} J$ versus $1/F$ plot of the emission current in our model for epoxy-graphite PFE material. The black dots are experimental points from Tuck *et al* [44]. The solid curve is our result which is given in equation (88) with $|\gamma(\omega_s)|F_b/2 = 1$; the dotted curves just above and below have $|\gamma(\omega_s)|F_b/2 = 2$ and 0.5 respectively. The straight line dashed curve is the FN-JWKB result with a field enhancement factor of 50. J is in units of A cm^{-2} and F is in units of V μm^{-1}. The work function $\varphi = 2.0$ eV, with $\mu = 0.323$ eV and $\sigma = 0.1$.

quasi-stationary assumption) underpins the whole theory and is also responsible for the short-range behaviour of the image potential. We find it very hard to go beyond this approximation without a microscopic theory that connects x_0, the inelastic processes, the resonance criterion and the quasi-stationary assumption. Finally, the penultimate current expression:

$$J = \frac{me\varphi^2}{2\pi^2\hbar^3}\int_{-\delta}^{0} T(\varphi x)\frac{k_B T}{\varphi}\ln\left(1+\exp\left[-\frac{\varphi x}{k_B T}\right]\right)\mathrm{d}x, \tag{87}$$

and its subsequent temperature behaviour (see equation (44) in [1]) assumes the one-sided resonance characteristic of the Drude type model, as mentioned in comments after equation (36) in section 4 above. It is still unclear what will emerge in a more sophisticated model, where the temperature dependence of $\kappa(\omega)$ is considered; this is worth further exploration. More investigations of these questions will be motivated by a closer study of both the temperature and energy distribution of the emission current in experiments.

For now we can relate the important parameter $\gamma(\omega_s)$ (see section 5) to the current J, which to leading order is given by:

$$J_{CH} \approx \frac{c_A\varphi^{-3/2}}{[\ln(\frac{c_B\varphi}{(eF)^{1/2}})]^2}\left(\frac{|\gamma(\omega_s)|F_b}{2}\right)^{3/4}\sqrt{\frac{\mu}{\varphi}}(eF)^3 \qquad \text{A cm}^{-2}, \tag{88}$$

where the constants are $c_A = 0.099\,24$ eV$^{-3/2}$ μm^3 and $c_B = 51.231$ eV$^{-1/2}$ μm$^{-1/2}$ respectively (see equation (46) of our earlier paper [1]). Since $\gamma(\omega_s)$ is measurable via THz surface spectroscopy including pump–probe polarization techniques [38], this formula provides a means to classify and to some extent optimize the emission current of the carbon surface where the ideal surface would have $|\gamma(\omega_s)| \geqslant 2F_b$ (see equation (43)). Figure 2 shows the results of this model in comparison with experimental results for an epoxy–graphite material.

9. Conclusion

The present work provides a more quantitative formulation of the key ideas for dynamically enhanced resonant tunnelling which sets the carbon field emitters apart from the usual FN theory

which applies to metals in general. By careful re-examination of the salient features of the time-dependent Schrödinger equation, we have isolated and clarified the main assumptions in the dynamical theory; many of these assumptions are already intrinsic to traditional field emission theory. In principle our theory indicates opportunities for the control of field emission. The main parameters are the work function φ which controls the barrier, the Fermi level, namely μ which controls the plasmon frequency, and $\gamma(\omega_s)$ which controls the resonance peak. However, we have found that the anharmonicity of the surface plasmon modes, i.e. anharmonic coefficient a, and an underlying characteristic frequency ω_0, are essential components which, due to their influence on the non-linear susceptibility $\gamma(\omega_s)$, couple both static and dynamic fields. These are necessary ingredients for a more accurate description of the resonance behaviour. When other dissipative mechanisms such as collision damping parameter Γ and non-linear dissipative feedback (see section 7) are diminished, these parameters make carbon systems different from traditional metals. Such damping effects set an upper limit for the relaxation time of the order of picoseconds, a unique feature of carbon-based systems which have high mobilities and supported by time domain studies of electron–phonon scattering in SWCNTs [45]. Indeed, since our study merely stopped at the second-order susceptibility, it is possible that, as the field increases, higher-order susceptibilities come into play, explaining the characteristic break in the field as found in some CNT systems. In that context, recent suggestions of two-process models, which are inherently time dependent in their very nature, should be carefully re-examined using the time-dependent theory as presented here, in view of the neglect of time-dependent and relaxation processes by the authors [46, 47].

While it will be foolish to think that the present work has completely validated the earlier phenomenological model [1], the studies here do provide confidence that important physics concerning dynamical enhancement of tunnelling due to the surface properties of carbon field emitters has been identified. Further work remains to examine the microscopic properties alluded to, and experiments should be focused on a more systematic analysis of the resonance and dynamical current characteristics. In addition to improving field emission, these studies should provide unique opportunities for the exploitation of non-linear plasmon modes for THz applications in the range of several hundred THz. With some generalizations, including the extension to more than one dimension, the present model could make possible the design of systems with greatly enhanced electron emission, and might even allow control of the emission direction.

Acknowledgments

The authors are grateful to the Engineering and Physical Sciences Research Council for financial support under grants GR/M71404/01, GR/S23506/01 and GR/R97047/01.

References

[1] Choy T C, Harker A H and Stoneham A M 2004 *J. Phys.: Condens. Matter* **16** 861–80
[2] Fowler R H and Nordheim L W 1928 *Proc. R. Soc.* A **119** 173–81
[3] Nordheim L W 1928 *Proc. R. Soc.* A **121** 626–39
[4] Gao H, Mu C, Wang F, Xu D, Wu K, Xie Y, Liu S, Wang E, Xu J and Yu D 2003 *J. Appl. Phys.* **93** 5602–5
[5] Murakami H, Hirakawa M, Tanaka C and Yamakawa H 2004 *Appl. Phys. Lett.* **76** 1776–8
[6] Zhi C Y, Bai D and Wang E G 2004 *Appl. Phys. Lett.* **81** 1690–2
[7] Landau L D and Lifshitz E M 1991 *Quantum Mechanics (Non-Relativistic Theory)* 3rd edn (Oxford: Pergamon) p 55 (section 18)
[8] Jonson M 1980 *Solid State Commun.* **33** 743–6
[9] Mahan G D 1993 *Many-Particle Physics* 2nd edn (New York: Plenum) pp 629–34 (section 7.1)

[10] Mills D L 2002 *Phys. Rev.* B **65** 077404
[11] Landau L D, Lifshitz E M and Pitaevskii L P 1984 *Electrodynamics of Continuous Media* 2nd revised edn (Oxford: Pergamon) pp 279–83 (section 82)
[12] Joynt R 1999 *Science* **284** 777–9
[13] Mills D L 2000 *Phys. Rev.* B **62** 11197–202
[14] Joynt R 2002 *Phys. Rev.* B **65** 077403
[15] Mills D L 1977 *Phys. Rev.* B **15** 763–70
[16] Landau L D and Lifshitz E M 1991 *Quantum Mechanics (Non-Relativistic Theory)* 3rd edn (Oxford: Pergamon) pp 56–7 (section 19)
[17] Razavy M 2003 *Quantum Theory of Tunnelling* (Singapore: World Scientific) pp 149–81
[18] Tran Thoai D B and Šunjić M 1991 *Solid State Commun.* **77** 955–9
[19] Persson B N J and Baratoof A 1988 *Phys. Rev.* B **38** 9616–28
[20] Šestović D, Marušić L and Šunjić M 1997 *Phys. Rev.* B **55** 1741–7
[21] Arafune R, Hayashi K, Ueda S and Ushioda S 2004 *Phys. Rev. Lett.* **92** 247601
[22] Landau L D, Lifshitz E M and Pitaevskii L P 1984 *Electrodynamics of Continuous Media* 2nd revised edn (Oxford: Pergamon) pp 358–62 (section 103)
[23] Mills D L and Evans E 1973 *Phys. Rev.* B **8** 4004–18
[24] Berestetskii V B, Lifshitz E M and Pitaevskii L P 1980 *Quantum Electrodynamics* 2nd edn (Oxford: Pergamon) p 15 (section 5)
[25] Casimir H B and Polder D 1948 *Phys. Rev.* **73** 360–72
[26] Schaich W L 1981 *Phys. Rev.* B **24** 686–91
[27] Modinos A 1984 *Field, Thermionic, and Secondary Electron Emission Spectroscopy* (New York: Plenum) chapter 5
[28] Ritchie R H and Marusak A L 1966 *Surf. Sci.* **4** 234–40
[29] Newns D 1970 *Phys. Rev.* B **1** 3304–22
[30] Mele E J 2001 *Am. J. Phys.* **69** 557–62
[31] Landauer R and Martin Th 1994 *Rev. Mod. Phys.* **66** 217–28
[32] Sze S M 1981 *Physics of Semiconductors* 2nd edn (New York: Wiley) pp 254–65 and references quoted therein
[33] Harris J and Jones R O 1973 *J. Phys. C: Solid State Phys.* **6** 3585–604
[34] Ohanian H 1990 *Am. J. Phys.* **51** 1020–2
[35] Bochive E J and Walkup J F 1990 *Am. J. Phys.* **58** 131–4
[36] Mikheev G M and Zonov R G 2004 *Appl. Phys. Lett.* **84** 4854–6
[37] Landau L D, Lifshitz E M and Pitaevskii L P 1984 *Electrodynamics of Continuous Media* 2nd revised edn (Oxford: Pergamon) pp 374–8 (section 108)
[38] Svirko Yu P and Zheludev N I 2000 *Polarization of Light in Non-Linear Optics* (New York: Wiley)
[39] Shen Y R 2003 *The Principles of Non-Linear Optics* (New York: Wiley)
[40] Jordan D W and Smith P 1987 *Non-Linear Ordinary Differential Equations* (Oxford: Clarendon)
[41] Mahan G D 1993 *Many-Particle Physics* 2nd edn (New York: Plenum) p 394 (section 5.1)
[42] Flynn C P and Stoneham A M 1970 *Phys. Rev.* B **1** 3966–78
Flynn C P and Stoneham A M 1971 *Phys. Rev.* B **3** 2819
[43] Landau L D and Lifshitz E M 1991 *Quantum Mechanics (Non-Relativistic Theory)* 3rd edn (Oxford: Pergamon) pp 148–51 (section 41)
[44] Tuck R A, Taylor W and Latham R V 1997 *Proc. 4th Int. Display Workshop* (Nagoya: Society for Information Display) pp 723–6
[45] Hertel T and Moos G 2000 *Phys. Rev. Lett.* **84** 5002–5
[46] Altman I S, Pikhitsa P V and Choi M 2004 *Appl. Phys. Lett.* **84** 1126–8
[47] Altman I S, Pikhitsa P V and Choi M 2004 *J. Appl. Phys.* **96** 3491–3